

# Percolation-dependent Reaction Rates in the Etching of Disordered Solids

K. M. Kolwankar <sup>1,2</sup>, M. Plapp <sup>2</sup> and B. Sapoval <sup>1,2</sup>

<sup>1</sup> *Centre de Mathématiques et de leurs Applications, Ecole Normale Supérieure - CNRS, 94140 Cachan, France*

<sup>2</sup> *Laboratoire de Physique de la Matière Condensée, Ecole Polytechnique - CNRS, 91128 Palaiseau, France*

A prototype statistical model for the etching of a random solid is investigated in order to assess the influence of disorder and temperature on the dissolution kinetics. At low temperature, the kinetics is dominated by percolation phenomena, and the percolation threshold determines the global reaction time. At high temperature, the fluctuations of the reaction rate are Gaussian, whereas at low temperature they exhibit a power law tail due to chemical avalanches. This is an example where microscopic disorder directly induces non-classical chemical kinetics.

Pacs: 64.60.Ak, 82.20.-w, 61.43.-j, 05.65.+b

Chemical etching of disordered solids is a process of great practical importance [1]. In some cases, such as in corrosion, it can be a cause of undesirable deterioration. In other cases it is useful, for example when one wishes to roughen a smooth surface for adhesion or to obtain some specific optical or esthetic properties. Such processes are also stimulating from a theoretical point of view since it has been observed in experiments [2,3,4] that they can give rise to complex patterns and dynamics.

To understand the universal features of random etching processes, the study of simplified toy models is useful since they allow to grasp some essential results using the concepts of percolation theory [5]. The randomness of the solid may be caused either by the topology of the chemical bonds, such as in amorphous media, or by fluctuations of the composition, such as in a solid solution. It can also be the randomness of a passivation layer that may appear spontaneously in the corrosion of polycrystalline solids.

In this letter, we focus on the time evolution of the etching process and the influence of temperature. In the previous studies of random etching, random site *resistances* were assigned, and “strong” sites were never etched [6,7,8]. This has given a theoretical interpretation to the spontaneous stabilization of fractal surfaces in a model where the etchant is consumed in the course of the reaction [6,7,8]. The fluctuations observed in [2] were interpreted in terms of a self-organized fractal growth linked to percolation theory [7].

However, if the disorder is at some microscopic level, it is more realistic to assign random *reaction rates* to the dispersed random elements of the solid. Then, even a site with a very small dissolution rate will eventually be etched. Furthermore, since real reaction rates are temperature-dependent, the influence of this parameter

can be studied. In the following, we find a transition from smooth and continuous growth at high temperatures to a highly intermittent regime at low temperatures that exhibits chemical avalanches.

The 2d square lattice model of the solid consists of elements  $i$  that have a random site-dependent binding energy  $E_i$ . The dissolution rate  $R_i$  of a molecule  $i$  in contact with the etchant is supposed to follow an Arrhenius law that corresponds to an activated process:

$$R_i = C \omega_0 \exp(-E_i/k_B T), \quad (1)$$

where  $C$  is the concentration of the etchant,  $k_B$  is Boltzmann’s constant, and  $T$  is the temperature. For simplicity, the attempt frequency  $\omega_0$  is assumed to be the same for all sites. The energies  $E_i$  are supposed to be distributed over a finite range. The simplest choice is  $E_i = E_0 + p_i \Delta E$  where the  $p_i$ ’s are distributed uniformly between 0 and 1. Then, Eq. 1 can be rewritten as

$$R_i = C \omega \exp(-E_\beta p_i), \quad (2)$$

where  $\omega = \omega_0 \exp(-E_0/k_B T)$  and  $E_\beta = \Delta E/k_B T$ . Note that this simplified model neglects many factors that may affect real dissolution rates, such as for example steric blocking. There are essentially two limits depending on the value of  $E_\beta$ . With  $k_B T$  of order 25 meV at room temperature, weak disorder (“high temperature”) typically corresponds to  $E_\beta$  of order unity, and strong chemical disorder (“low temperature”) corresponds to  $E_\beta$  of order 10 to 100.

We consider an irreversible reaction with no redeposition, and we suppose that one molecule of etchant is consumed per dissolved site. It follows that for a finite volume of etchant with initially  $N$  etchant molecules and concentration  $C_0$ , the concentration after the dissolution of  $j$  sites is  $C_j = C_0(1 - j/N)$ . It therefore decreases with time, and the reaction stops when all the etchant molecules are exhausted. Furthermore, we suppose that the mixing in the solvent (by diffusion of the etchant or hydrodynamic flow) is fast compared to the chemical events, such that the concentration in the solution remains uniform.

The time evolution of etching is studied through an event-oriented Monte Carlo algorithm in physical time. A site  $i$  dissolves within a time interval  $\Delta t$  with probability  $R_i \Delta t$  if  $\Delta t$  is small enough ( $R_i \Delta t \ll 1$ ). Since these probabilities are independent for different sites, the probability that *any* of the surface sites is etched in the time interval  $\Delta t$  is  $\sum_{i \in S} R_i \Delta t$ , where the sum runs over all the

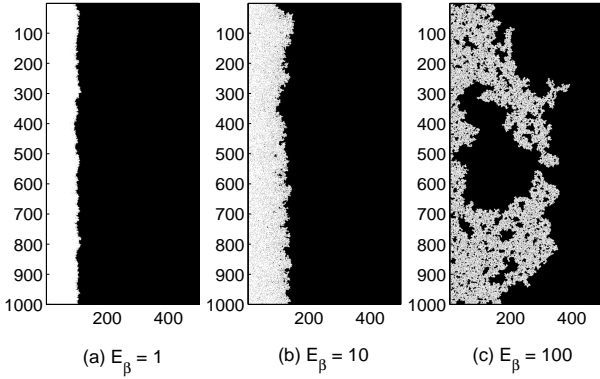


FIG. 1. Snapshot pictures of the etching front at the end of the reaction for  $N = 10^5$ ,  $L = 10^3$  and (a)  $E_\beta = 1$ , (b)  $E_\beta = 10$  and (c)  $E_\beta = 100$ . The unetched solid is black and the solution is white. Note that the surface of the white regions is the same and equal to  $N$ , the initial number of etchant molecules in the solution.

surface particles (active sites). The time interval before a site is etched with probability one is therefore

$$\Delta t = \frac{1}{\sum_{i \in S} R_i} = \frac{1}{C\omega \int_0^1 h(p) \exp(-E_\beta p) dp}, \quad (3)$$

where  $h(p)$  gives the number of active sites with resistance between  $p$  and  $p + dp$ . Within that time interval, a given site  $i$  is etched with probability

$$P_i = \frac{R_i}{\sum_{i \in S} R_i} = \frac{\exp(-E_\beta p_i)}{\int_0^1 h(p) \exp(-E_\beta p) dp}. \quad (4)$$

In each Monte Carlo step, the algorithm chooses to etch a surface site  $i$  with probability  $P_i$  and increases the time  $t$  by  $\Delta t$ . As a consequence, the physical time is *not proportional* to the number of Monte Carlo steps, since  $\Delta t$  depends on the dissolution rates of all the surface sites. However, by construction, the average time needed to dissolve a *given* site with reaction rate  $R_i$  is always the same, independently of the system size or the surface configuration. The probability distribution of Eq. 4 has already been used in Ref. [9] to study the influence of finite temperature on invasion percolation, but this study was restricted to the initial stages of the process.

The initial lattice of width  $L$  has a flat interface. The ratio  $N/L$  is the etching depth if uniform dissolution occurs. We study here the case  $N/L \gg 1$  such that deep pores can be formed. In this situation, the essential parameter that governs the pattern formation is the reduced energy  $E_\beta$  which controls the relative dissolution speed of “hard” and “weak” sites. For small  $E_\beta$ , the dissolution rate is nearly the same for all sites whatever their energy; in the limit  $E_\beta \rightarrow 0$ , this model maps onto the Eden model [10]. In this regime, etching leads to the formation of a microscopically rough, but macroscopically smooth interface that has a finite width  $W$  and propagates with a roughly constant speed (Fig. 1a). When

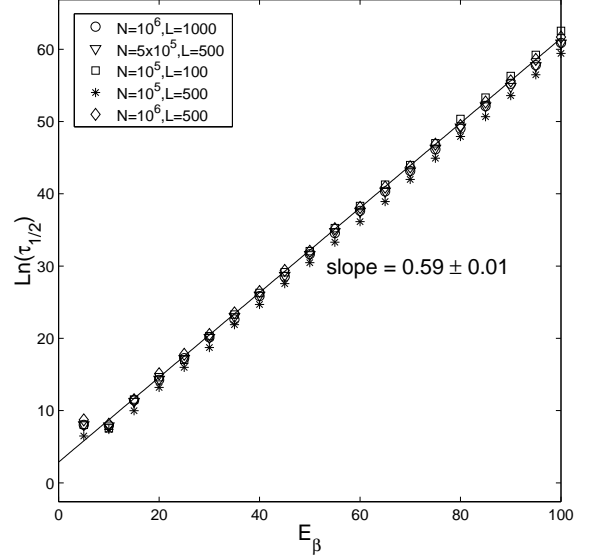


FIG. 2. Activation plot of the reaction half-time  $\tau_{1/2}$ .

$E_\beta$  increases, sites with small  $p_i$  become relatively much faster than sites with large  $p_i$ . The dynamics leads to a irregular or porous interface (Figs. 1b and 1c), with disconnected islands surrounded by sites which may survive for a long time. These islands continue to be slowly etched and their size therefore decreases with time. In the limit  $E_\beta \rightarrow \infty$ , the weakest site is chosen with probability 1 and the model becomes identical to classical invasion percolation [11].

For this reason, it is not surprising that the percolation properties of the underlying lattice enter the dynamics in the large  $E_\beta$  limit. Our main focus here is the chemical kinetics. The global reaction rate strongly depends on temperature. To characterize its behavior, we show in Fig. 2 the reaction half-time  $\tau_{1/2}$ , that is, the time it takes to consume half of the  $N$  etchant molecules, as a function of  $E_\beta$ . For large enough  $E_\beta$ , this plot gives an effective activation energy equal to  $(0.59 \pm 0.01)$ , close to the square lattice percolation threshold  $p_c$ . The time for the reaction to go from  $N/2$  to  $N/4$  etchant molecules follows the same behavior. Simulations for the 3D cubic lattice give a similar result with a slope  $0.30 \pm 0.01$ , close to  $p_c$  for this 3D lattice. This indicates that, for strong disorder (or low temperature) the global reaction has an activation energy equal to  $E_0 + p_c \Delta E$  (the  $E_0$  contribution comes from the definition of  $\omega$ ). To our knowledge, this is the first direct appearance of a percolation threshold in the *time domain*.

Figure 3 shows the histograms  $h(p)$  of the site resistances  $p_i$  on the solid-liquid interface (including the islands) after 50% of the etchant is consumed for different temperatures. They count the number of surface sites with  $p < p_i < p + \epsilon$  as a function of  $p$  (here  $\epsilon = 0.01$ ).

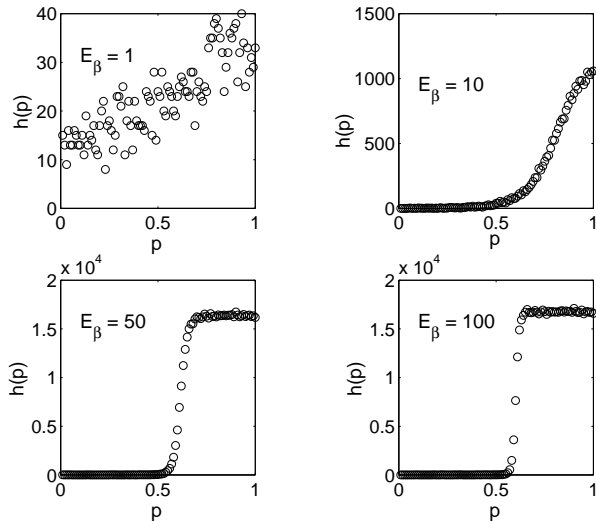


FIG. 3. Histogram of  $p_i$ s on the interface after 50% of the etchant is consumed (averaged over 10 realisations). Here,  $N = 10^6$ ,  $L = 10^3$ .

For small  $E_\beta = 1$  (high temperature),  $h(p)$  increases with  $p$ , but there is always a large number of weak sites on the surface. In contrast, for  $E_\beta \gg 1$  (low temperature), there are very few weak sites, and  $h(p)$  starts to increase sharply at a value close to the percolation threshold.

These data help to explain the appearance of the percolation threshold in the reaction rate. The total time needed to etch  $n$  molecules is simply the sum of the time-steps for each individual etching event,  $t = \sum_{j=1}^n \Delta t_j$ . At high temperature, all the dissolution rates are of similar magnitude. Therefore, the time-step depends only weakly on the surface configuration and the reaction proceeds with a well-defined average rate. In contrast, at low temperature, the contributions of successive configurations are very different. For a typical configuration that contains a few weak sites, the sum in the denominator of Eq. (3) is dominated by the large rates associated with these sites, the corresponding time-step is small, and the weakest site is etched with a probability close to one. However, from time to time, the growth front coincides with the perimeter of a percolation cluster. In this situation, the weakest site has a strength close to  $p_c$ , and the corresponding time-step scales as  $\Delta t \sim \exp(E_\beta p_c)$ . As a consequence, the dynamics consists of series of rapid etching events (“chemical avalanches”) separated by long time steps when the front has reached the surface of a percolation cluster. The appearance of the percolation threshold in the reaction time indicates that the latter are the rate-limiting steps.

The time evolution of the histograms can be qualitatively understood on a coarse-grained time scale, that is, a time scale much larger than individual time-steps. On this scale, one can define a global reaction rate  $R$ , that is, the total number of sites etched per unit time. Note that  $R$  must be proportional to  $C\omega$ . One can then write a

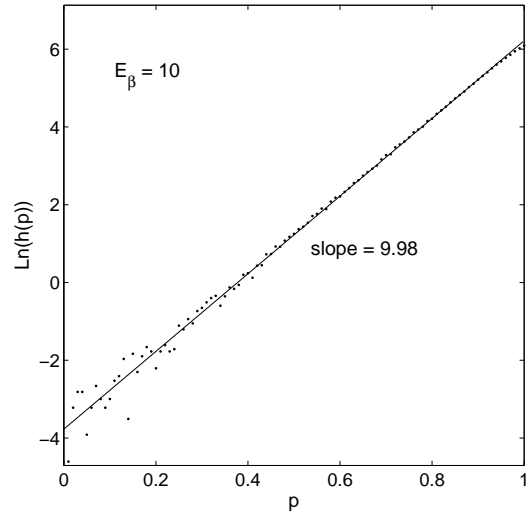


FIG. 4. Histogram of  $p_i$ s on the *final* interface for  $E_\beta = 10$ ,  $N = 10^6$  and  $L = 10^3$ .

continuous evolution equation for the number of surface sites of strength  $p$ :

$$\frac{dh(p)}{dt} = R\epsilon - h(p)C\omega \exp(-E_\beta p). \quad (5)$$

The first term counts the arrival of freshly uncovered sites (with uniform distribution) on the surface, whereas the second term is the product of the etching rate of sites with strength  $p$  times their number. One clearly sees that  $h(p) = R\epsilon \exp(E_\beta p)/(\omega C)$  is a steady-state solution of this equation. This is indeed what is observed for high temperatures. For low temperatures, inserting  $R \sim C\omega \exp(-E_\beta p_c)$  yields  $h(p) \sim \epsilon \exp[E_\beta(p - p_c)]$  [12], in remarkable agreement with the *final* histogram data for  $E_\beta = 10$ , shown in Fig. 4. This has a general consequence that could be called the “chemical survival of the fittest”: since almost all weak sites have been removed from the surface, the disordered solid is stronger once etched than it was before the attack. This has already been discussed in a simpler context [8].

One notes that, for even lower temperatures, the *transitory*  $h(p)$  shown in Figure 3 levels off for large  $p$ . This occurs because in our simulations the total number of steps is far too small to reach the steady state at low temperature. Indeed, for such a steady state to appear, a sufficient contrast must occur between sites above  $p_c$ . For this to happen, a huge number of strong sites must be uncovered, and this requires an exceedingly long time. At zero temperature, which is equivalent to invasion percolation, the steady state is never reached. The plateau for the highest  $p$  values in the transitory histograms simply reflects the initial uniform distribution of site strengths.

The chemical avalanches that occur at low temperatures can be characterized in two different ways. The first is purely geometric. When the “hard” perimeter of a percolation cluster is broken, the reaction has a large

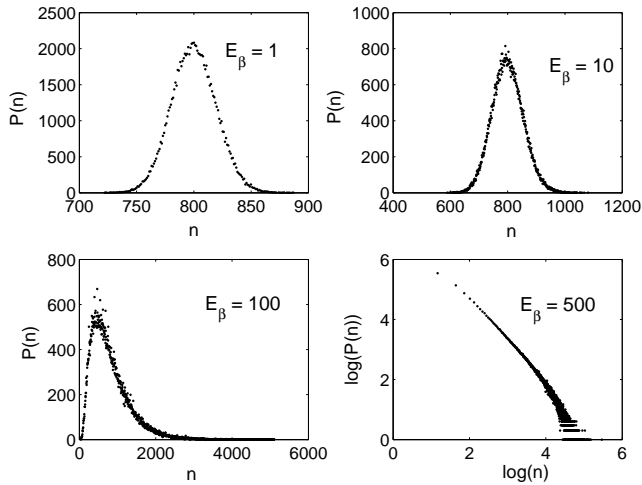


FIG. 5. Statistical distribution of the reaction rate for different temperatures: distribution of the number  $n$  of sites etched in a time interval  $t_2 - t_1 = T_{tot}/1000$ . Here  $N = 10^6$ ,  $L = 10^3$ . The first 20% of events have been discarded.

probability to continue at the place where the last etching event has occurred since new weak sites may be uncovered. The avalanche size can then be determined by “connected cluster events”. Starting with a given etching event, if the next etched site is a first neighbor, it is added to the cluster, and so on, until the next etched site is not a neighbor to any of the cluster sites. For large values of  $E_\beta$ , the number of avalanches versus their size follows a power law with a slope around  $1.53 \pm 0.01$  (not shown here), in agreement with the result for classical invasion percolation [13].

A more physical way to characterize avalanches is via the global reaction rate. It can be written as

$$R = \frac{n(t_2 - t_1)}{t_2 - t_1}, \quad (6)$$

where  $n(t_2 - t_1)$  is the number of sites etched between times  $t_1$  and  $t_2$ . So defined, this quantity is proportional to an experimental signal, for example the corrosion current if the etching is the result of an electrochemical process. To study the behavior of the reaction rate, we have performed simulations with a constant etchant concentration  $C$  (corresponding to an infinite volume of solution) up to a fixed number of etched sites  $N$ . The total reaction time  $T_{tot}$  was divided in equal time intervals  $t_2 - t_1 = T_{tot}/1000$ , and the number of sites etched in each interval was counted (discarding the initial etching of the flat surface). The resulting histograms are shown in Fig. 5. For small  $E_\beta$  values, the reaction rate has a Gaussian distribution around a well-defined average. In contrast, for very large values of  $E_\beta$ , the histogram becomes close to a power law due to the occurrence of avalanches with a broad size distribution. Therefore, the reaction rate has large fluctuations in both space and time. Recently, chemical avalanches have been found in

experiments [3] and were explained in terms of a sand-pile model [14]. Our findings might offer an alternative interpretation for these observations.

In summary, we have introduced a minimal model for the etching of a disordered solid. We have studied the influence of temperature on chemical kinetics and etching patterns. At high temperature (or weak disorder), the reaction rate exhibits gaussian fluctuations around a well-defined average rate, and the dissolution front is macroscopically smooth. At low temperature (or strong disorder), the reaction rate has strong fluctuations caused by chemical avalanches. The global reaction rate is shown to depend on temperature with an activation energy directly related to the percolation threshold. Interestingly, the avalanches, which may be large at low temperature, do not influence the reaction rate itself. The effect of possible redeposition and that of concentration gradients on reaction kinetics and patterns should be examined in the future.

- 
- [1] U. R. Evans, *The corrosion and Oxidation of Metals: Scientific Principles and Practical Applications*, Arnold, (London), 1960). H. H. Uhlig, *Corrosion and Corrosion Control*, (Wiley, New York), 1963.
  - [2] L. Balázs, Phys. Rev. E **54**, 1183 (1996).
  - [3] J. R. Claycomb et. al., Phys. Rev. Lett., **87**, 178303, (2001).
  - [4] A. Legat and V. Dolecek, J. Electrochem. Soc., **142**, 1851, (1995).
  - [5] D. Stauffer and A. Aharony, *Introduction to Percolation Theory*, Taylor and Francis (London), 1994.
  - [6] B. Sapoval, S. B. Santra, and P. Barboux, Europhys. Lett., **41**, 297, (1998).
  - [7] S. B. Santra and B. Sapoval, Physica A **266**, 160 (1999).
  - [8] A. Gabrielli, A. Baldassarri, and B. Sapoval, Phys. Rev. E **62**, 3103 (2000).
  - [9] A. Gabrielli, G. Caldarelli and L. Pietronero, Phys. Rev. E **62**, 7638 (2000).
  - [10] A. L. Barabasi and H. E. Stanley, *Fractal Concepts in Surface Growth*, (Cambridge University press, Cambridge, 1995).
  - [11] D. Wilkinson and J. F. Willemsen, J. Phys. A **16**, 3365 (1983).
  - [12] This can also be deduced as a fixed point solution of a recurrence relation relating the histogram at the  $n$ th Monte Carlo step to that of  $(n + 1)$ th.
  - [13] S. Roux and E. Guyon, J. Phys. A: Math. Gen. **22**, 3693 (1989).
  - [14] P. Bak, C. Tang and K. Wiesenfeld, Phys. Rev. Lett. **59**, 381 (1987); Phys. Rev. A **38**, 364 (1988).